International Journal of Applied Mathematics
Volume 38 No. 10s, 2025
ISSN: 1311-1728 (printed version); ISSN: 1314-8060 (on-line version)

FINITE ELEMENT STUDY ON THE STABILITY OF HOMOGENEOUS AND LAYERED SOIL SLOPES UNDER STATIC AND SEISMIC LOADING

Julee Singh[1*], Sneha Gupta[2]

[1*]Research Scholar, Department of Civil Engineering, Madan Mohan Malaviya University of Technology, Gorakhpur, 273010, India
[2]Assistant Professor, Department of Civil Engineering, Madan Mohan Malaviya University of Technology, Gorakhpur, 273010, India

Abstract

This study investigates the stability of homogeneous and layered soil slopes under static and seismic loading using the strength reduction finite element method in OPTUM G2. Slopes of 6 m height with inclinations of 30°, 45°, and 60° were analysed using Mohr–Coulomb and Drucker–Prager models. For homogeneous slopes, the factor of safety decreased from 1.44 to 0.87 as slope angle increased, with further reductions of 15–20% under seismic loading ($K_h = 0.12$); differences between constitutive models were negligible for moderate slopes but reached about 5% for steep slopes. In layered slopes, minimum safety factor occurred when the weak layer was located near the lower slope region ($h/t \approx 2$), resulting in stability reductions of nearly 30% compared to homogeneous slopes, while seismic loading reduced sensitivity to layer position except near the crest. Soil nailing restored safety values to target of 1.5 (static) and 1.1 (seismic), needing longer nails for multilayer slopes. The uniqueness resides in the integrated evaluation of weak-layer position, constitutive modelling, and soil nailing optimization under combined loading using OPTUM G2.

Keywords: Soil Cohesion; Friction Angle; Slope Angle; Safety Factor; Optimization.

1. Introduction

Slope stability is a fundamental concern in geotechnical engineering due to its direct consequences for the safety and serviceability of civil infrastructure. Slope collapses may be triggered by rainwater infiltration, groundwater level fluctuations, external stress, degradation of soil shear strength, erosion, or topographic adjustments [1,2]. Numerous investigations have investigated slope stability using limit equilibrium techniques (LEM) and conventional finite element methods (FEM), revealing the importance of soil strength parameters, constitutive modelling, and reinforcing measures [3–14]. Despite these developments, integrated numerical studies that simultaneously address homogeneous and layered soil conditions, weak-layer location, material model selection, and seismic effects remain limited, particularly when applying advanced computing frameworks.

Soil nailing is a widely established passive reinforcement technique for slope stabilization and has shown successful across a broad variety of soil types [13,15,16]. Stability improvement is achieved through mobilization of frictional resistance along steel bars inserted within the passive zone, leading to increased shear resistance and controlled deformation [17–19]. Previous studies have demonstrated that the performance of soil-nailed slopes is determined by slope geometry and nail properties, including length, spacing, diameter, inclination [20,21]. While some researchers saw modest contribution from top nails in cohesive soils [22], others indicated that nails near the slope crest largely promote global stability, whereas lower nails are more effective in minimizing horizontal displacement [23]. Soil shear strength factors exhibit a major influence on the factor of safety, although elastic properties and nail head stiffness often have secondary effects [24–27]. Parametric investigations further reveal that increased nail length-to-diameter ratio, diameter, and nail density lead to greater slope stability [28–31]. Consequently, modern FEM platforms such as PLAXIS and OPTUM G2 have been widely applied to analyse soil–nail interaction and optimize reinforcement

Received: October 25, 2025

design [19,32,33].

Although homogeneous and two-layered slopes have been analysed using analytical, LEM, and FEM approaches [34–36], the influence of weak-layer location in layered slopes has not been systematically investigated using OPTUM G2. Given that layered soil profiles are more representative of natural ground conditions, such an investigation is both practical and necessary. Accordingly, this study applies the strength reduction finite element method in OPTUM G2 to evaluate the stability of homogeneous and layered soil slopes under static and seismic loading. The analysis quantifies the effects of slope angle (β) and weak-layer position (h/t) on factor of safety and failure mechanisms, compares Mohr–Coulomb and Drucker– Prager constitutive models, validates OPTUM G2 predictions against conventional FEM and LEM results [37], and identifies optimum soil nail parameters for improving the stability of critical slopes.

2. MODELLING OF SLOPES

2.1. Geometry model of slopes

Slope angles (β) 30°, 45°, and 60° were analysed to represent typical cut and natural slopes ranging from stable to marginally stable conditions, under static and seismic loading. Both homogeneous and layered soil profiles were considered to reflect idealised and realistic ground conditions. Two-dimensional homogeneous and layered slope models (h/t = 1), developed in OPTUM G2, are shown in fig 1 and fig 2, where h is the distance from the slope crest to the weak layer and t is the constant thickness of the weak layer.

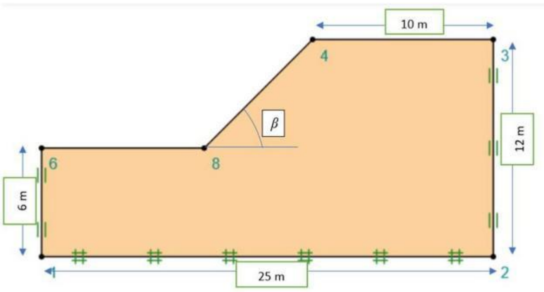

Figure 1: 2D model of homogeneous soil slopes (β=45°)

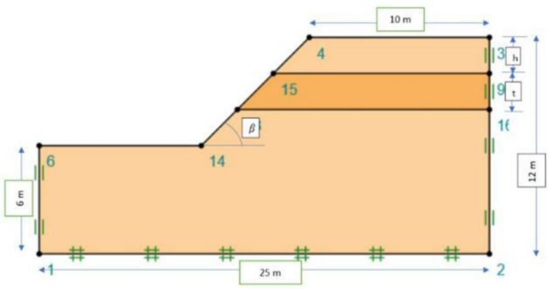

Figure 2: 2 D model of layered soil slope (h/t=1, β=45°)

2.2. Material properties

Soil properties were selected from well-established experimental and numerical studies to ensure realism and reproducibility, as summarized in table 1 [37]. Cohesion and friction angle values represent medium to stiff soils, while elastic parameters were chosen within commonly accepted ranges due to their secondary influence on global stability. Soil 1 was used for homogeneous slope analyses, whereas layered slopes were modelled using Soil 1 with Soil 2 introduced as a thin weak layer.

Table 1: Different soil properties assumed in this work [37]

Material	Unit weight (kN/m^3)	Angle of friction (°)	Soil cohesion (kN/m^2)	Young modulus (MN/m^2)	Poisson's ratio	Dilation angle (°)
Soil 1	20	18	10	8	0.3	0
Soil 2	20	10	6	8	0.3	0

2.3. Boundary and loading conditions

Two slope geometries were analysed. In both cases, horizontal displacements were restrained at the lateral boundaries, and the base was fully fixed. Analyses were performed under static (self-weight) and seismic loading conditions.

3. Methodology

Slope stability was evaluated using the strength reduction finite element method implemented in OPTUM G2 [38], in which soil cohesion and friction angle were progressively reduced until numerical failure occurred, and the corresponding reduction factor was taken as the factor of safety. Two-dimensional slopes with a constant height of 6 m and inclinations of 30°, 45°, and 60° were analysed for both homogeneous and layered soil conditions. In layered slopes, a thin weak layer was introduced at different locations defined by the ratio *h/t* to systematically examine its influence on stability. Analyses were carried out under static (self-weight) and seismic loading, with seismic effects represented by a horizontal seismic coefficient of 0.12g, while soil behaviour was modelled using Mohr–Coulomb and Drucker–Prager constitutive criteria. For slopes exhibiting inadequate stability, soil nailing was applied as a reinforcement measure, with nail material and diameter kept constant and nail length and spacing optimised to achieve target safety values of 1.5 under static loading and 1.1 under seismic loading. A mesh sensitivity study indicated that approximately 4000 elements ensured stable and accurate results, and this discretisation was adopted throughout the analyses.

4. Results and discussion

Results are reported as factors of safety for varying slope angles (β = 30°, 45°, 60°) and weak- layer positions (h/t = 0–3) under different soil models and loading conditions, with comparisons to previous studies. The main findings from the OPTUM G2 analyses are summarised below.

4.1Homogeneous Slopes: Stability trends and Failure mechanisms

The stability of homogeneous soil slopes analysed using OPTUM G2 shows a systematic decrease in factor of safety as slope angle increases from 30° to 60° under both static and seismic loading, reflecting the increasing dominance of driving forces over shear resistance, with seismic loading causing a more pronounced reduction due to inertial effects [36, 37]. As shown in table 2 and fig 3, fig 4, the Mohr–Coulomb model predicts slightly higher safety values for gentler slopes, whereas the Drucker–Prager model yields marginally higher values for steeper slopes, while both models give nearly identical results at 45°, indicating limited material-model sensitivity for intermediate geometries. Predicted failure is governed by deep- seated rotational slip surfaces initiating near the crest and extending towards the toe. The reliability of the OPTUM G2 results is confirmed by the close agreement with FEM and limit equilibrium methods, as demonstrated in table 3 and fig 5, while fig 6, fig 7, fig 8 collectively show that homogeneous soil slopes fail through similar deep-seated rotational mechanisms for slope angles of 30°, 45°, and 60°, with slip surfaces consistently initiating near the slope crest and propagating towards the toe. The close correspondence of failure surface shape and location predicted by OPTUM G2 with those obtained from FEM and limit equilibrium methods indicates that the failure mechanism is largely insensitive to slope angle within the investigated range and confirms the reliability of the numerical modelling approach [37].

Table 2: Comparison between MC and DP model for homogeneous slopes, using OPTUM G2

LOAD	**STATIC LOAD**			**SEISMIC LOAD**		
SLOPE ANGLE (β)	**30°**	**45°**	**60°**	**30°**	**45°**	**60°**
MC MODEL	1.435	1.09	0.8743	1.135	0.92005	0.76

Volume 38 No. 10s, 2025
ISSN: 1311-1728 (printed version); ISSN: 1314-8060 (on-line version)

DP MODEL	1.3905	1.0825	0.8932	1.123	0.93345	0.79

Table 3: Comparison of safety factor obtained by [37] with present solution for homogenous slope of 45° using OPTUM G2 (Static loading).

Different material model and method used	FOS
OPTUM G2	
Drucker-Prager	1.082
Mohr-Coulomb	1.092
GEO 5 [37]	
Drucker-Prager	1.17
Mohr- Coulomb	1.08
Bishop	1.09
Fellenius	1.06
Spencer	1.1

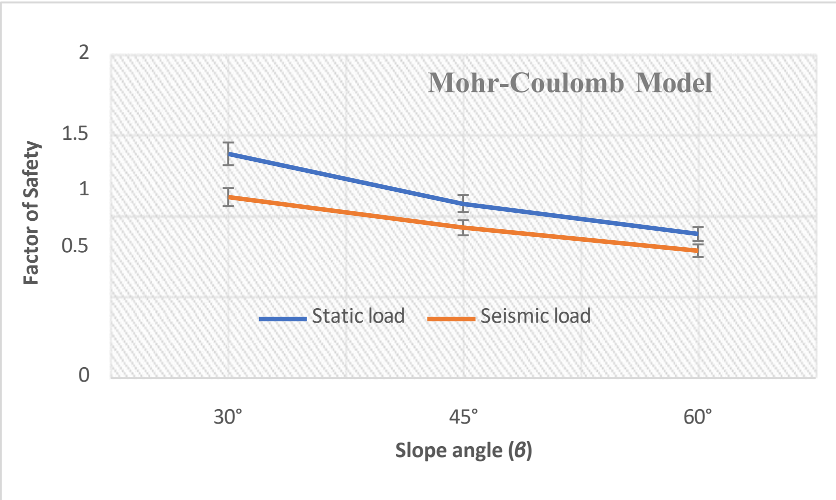

Figure 3: Variation safety factor with respect to slope angles for Mohr-Coulomb model.

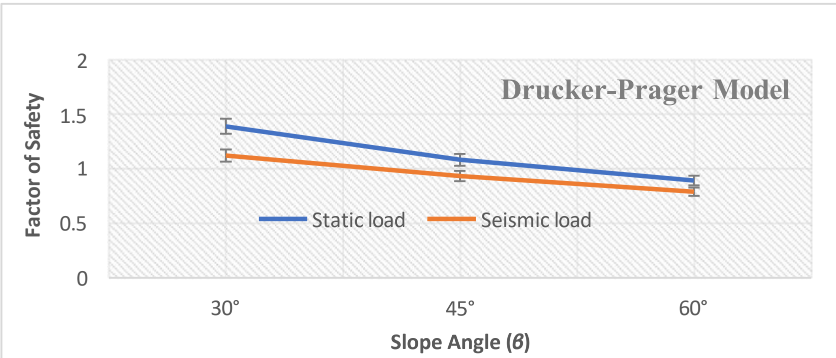

Figure 4: Variation of safety factor with respect to slope angles for Drucker-Prager model.

Received: October 25, 2025

International Journal of Applied Mathematics
Volume 38 No. 10s, 2025
ISSN: 1311-1728 (printed version); ISSN: 1314-8060 (on-line version)

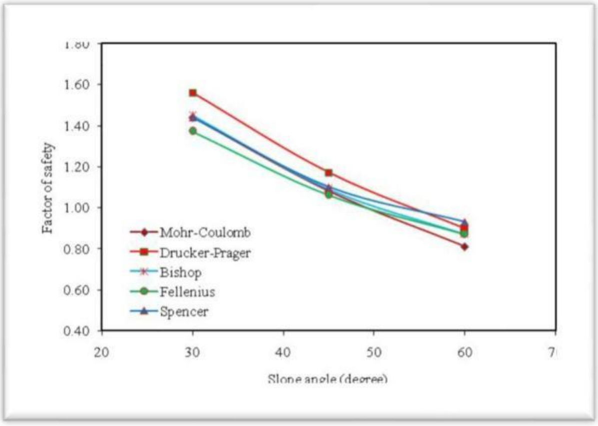

Figure 5: Variation of safety factor with respect to slope angles by different method [37]

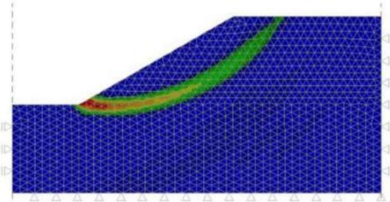

(a)

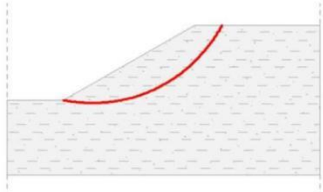

(b)

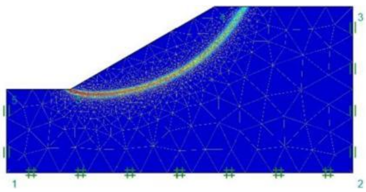

(c)

Figure 6: Comparison of failure surface by different methods for homogeneous soil slope of 30°: (a) FE (GEO5) [37] (b) LEM [37] (c) OPTUM G2

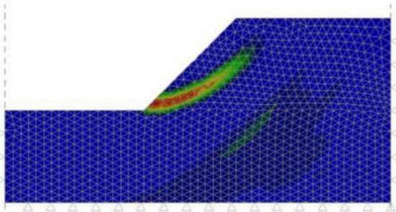

(a)

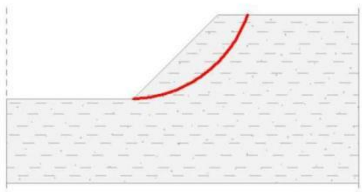

(b)

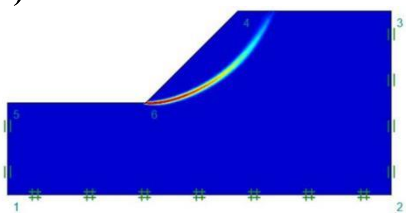

(c)

Figure 7: Comparison of failure surface by different methods for homogeneous soil slope of 45°: (a) FE (GEO5) [37] (b) LEM [37] (c) OPTUM G2

International Journal of Applied Mathematics
Volume 38 No. 10s, 2025
ISSN: 1311-1728 (printed version); ISSN: 1314-8060 (on-line version)

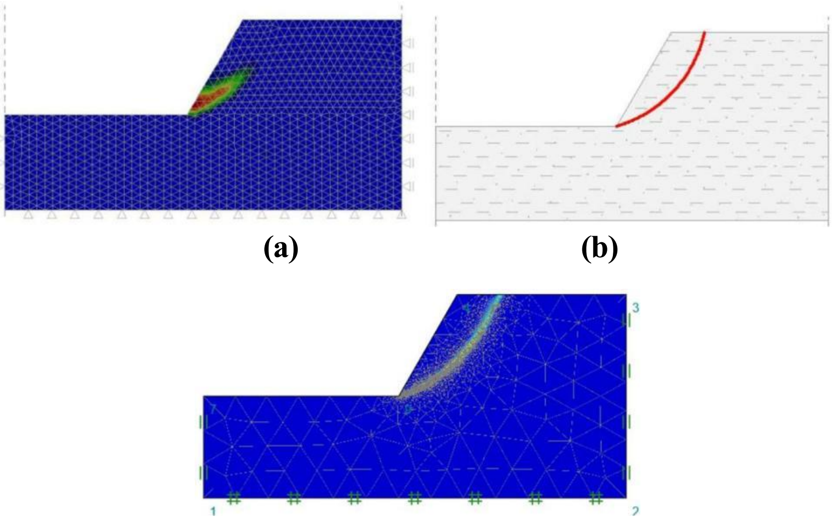

(a) (b)

(c)

Figure 8: Comparison of failure surface by different methods for homogeneous soil slope of 60°: (a) FE (GEO5) [37] (b) LEM [37] (c) OPTUM G2

4.2Layered Slopes: Influence of Weak-Layer Position

For layered slopes, stability is primarily governed by the position of the thin weak layer. Under static loading, the factor of safety decreases as the weak layer migrates downward from the crest, reaching a minimum when located near the lower portion of the slope ($h/t \approx 2$–3), beyond which stability improves slightly; this non-monotonic behaviour, evident from table 4 and fig 9, fig 10, is consistent across slope angles and constitutive models, indicating that weak layers intersecting the critical slip surface significantly reduce resistance. The Mohr–Coulomb model predicts marginally higher safety values for gentler slopes, whereas the Drucker–Prager model yields slightly higher values for steeper slopes, consistent with homogeneous slope behaviour. Under seismic loading, table 5 shows that factor values are uniformly lower and far less sensitive to weak-layer position, except when the weak layer is located at the crest ($h/t = 0$), where instability is most severe, demonstrating the dominance of seismic forces over stratification effects. Failure mechanisms, illustrated in fig 11, fig 12, fig 13, evolve from face and toe failures to basal sliding as the weak layer moves downward, with slip surfaces intersecting the slope face for shallow layers and transitioning to base failures for deeper layers. The close agreement between OPTUM G2 failure surfaces and those obtained from FEM and LEM analyses reported in the literature [36, 37] confirms the robustness and physical realism of the numerical framework.

Table 4: Comparison of safety factor for different slope angles of layered soil by OPTUM G2 (Static loading)

h/t	**Material model**	**Slope angles *(β)***		
		30°	**45°**	**60°**
0	MC	1.3755	1.0305	0.81615
	DP	**1.345**	**1.0315**	**0.84065**
1	MC	1.153	0.8999	0.74285
	DP	**1.1455**	**0.9047**	**0.7672**
2	MC	0.9879	0.76265	0.6249

ISSN: 1311-1728 (printed version); ISSN: 1314-8060 (on-line version)

	DP	**0.98705**	**0.78455**	**0.6656**
3	MC	1.056	0.8969	0.7923
	DP	**1.0535**	**0.90695**	**0.81575**

Table 5: Comparison of safety factor for different slope angles of layered soil (*h/t*=0) by OPTUM G2 (Seismic loading)

h/t	**Material model**	**Slope angles (*β*)**		
		30°	**45°**	**60°**
0	MC	1.142	0.9081	0.7430
	DP	1.1285	0.9213	0.7789

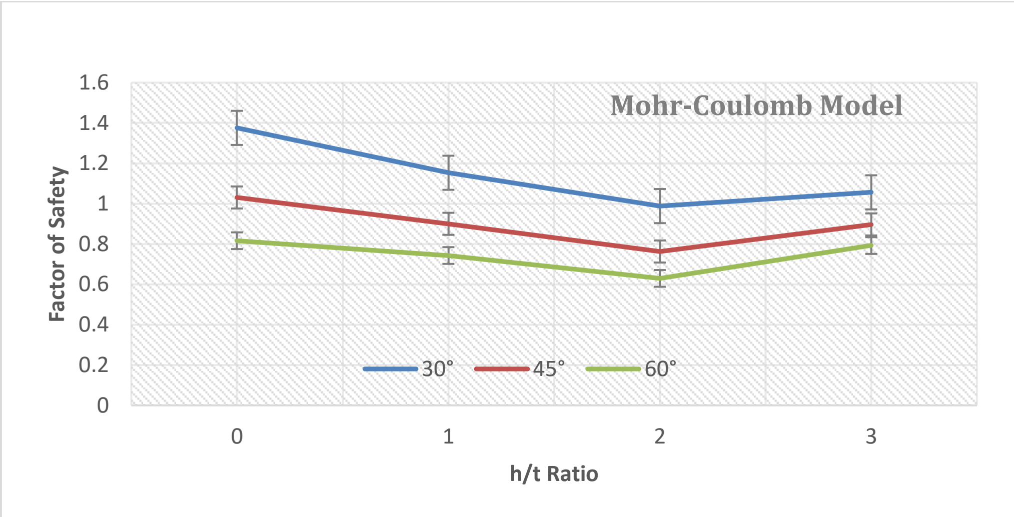

(a)

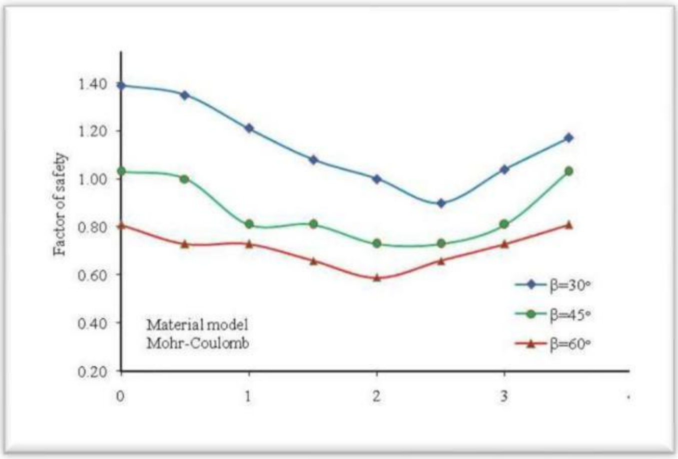

(b)

Received: October 25, 2025

Figure 9: Comparison of Variation of soil layer on safety factor of layered slopes for Mohr-Coulomb model (Static load) by different methods; (a) OPTUM G2 (b) FEM and LEM [37]

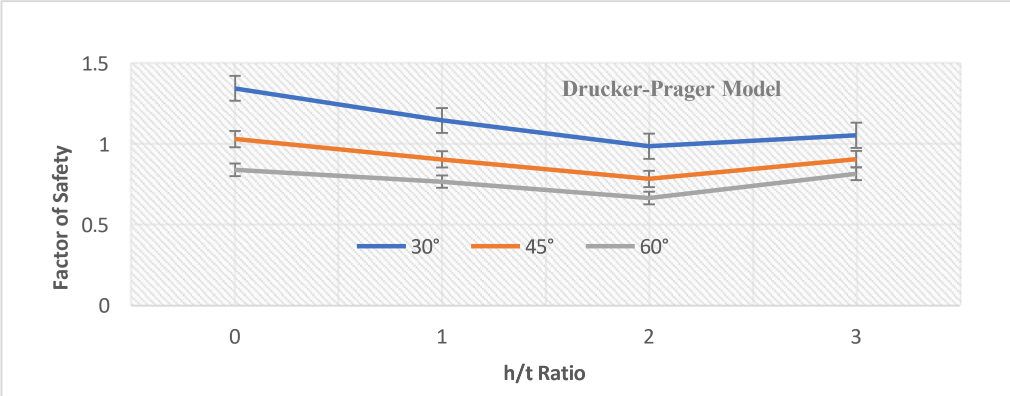

(a)

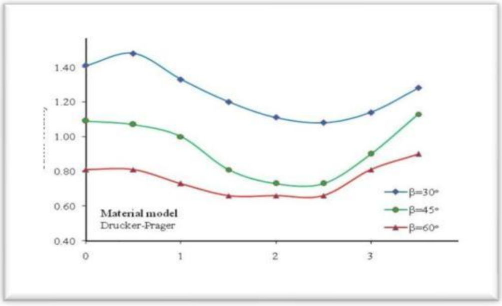

(b)

Figure 10: Comparison of Variation of soil layer on safety factor of layered slopes for Drucker- Prager model (Static load) by different methods; (a) OPTUM G2 (b) FEM and LEM [37]

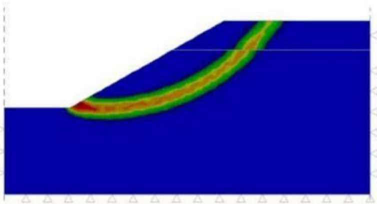

(a)

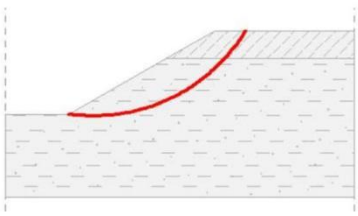

(b)

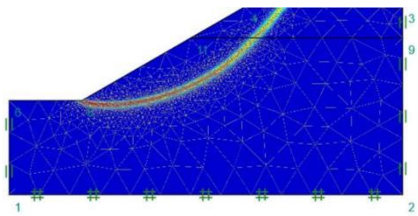

(c)

Figure 11: Comparison of failure surface by different methods for layered soil slope (Static load) of 30° and *h/t*=0: (a) FEM [37] (b)LEM [37] (c) OPTUM G2

Volume 38 No. 10s, 2025
ISSN: 1311-1728 (printed version); ISSN: 1314-8060 (on-line version)

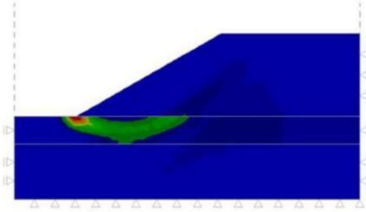
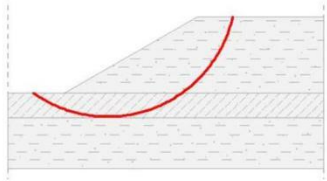

(a) **(b)**

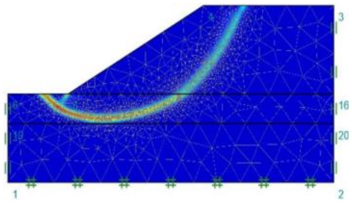

(c)

Figure 12: Comparison of failure surface by different methods for layered soil slope (Static load) of 30° and *h/t*=3: (a) FEM [37] (b)LEM [37](c) OPTUM G2

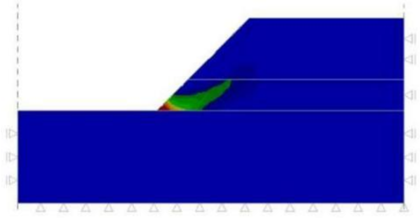
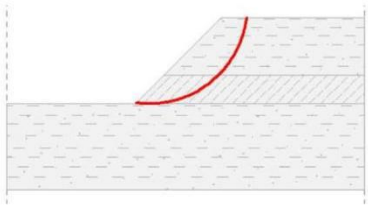

(a) **(b)**

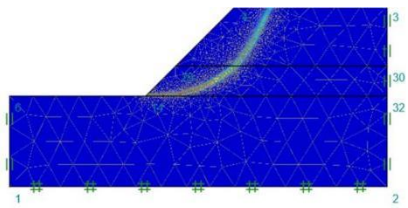

(c)

Figure 13: Comparison of failure surface by different methods for layered soil slope (Static load) of 45° and *h/t*=2: (a) FEM [37] (b) LEM [37](c) OPTUM G2

4.3Soil Nailing: Optimum Design and Stabilisation Mechanism

Soil nailing was applied to unstable homogeneous and layered slopes to restore stability to target safety levels (FoS = 1.5 under static loading and 1.1 under seismic loading), with the required reinforcement strongly influenced by slope geometry and stratification. As shown in table 6 and table 7, homogeneous slopes with steeper inclinations required shorter nail lengths and closer spacing to achieve the target safety values, indicating increased reliance on reinforcement mobilisation as failure mechanisms become more localised, consistent with earlier findings [27, 39]. For layered slopes with a weak layer at the crest (*h/t* = 0), table 8 and table 9 demonstrate that longer nails and tighter spacing were necessary compared to homogeneous slopes to achieve comparable stability. The stabilising mechanism is illustrated in fig 14, fig 15, fig16 where soil nailing alters the failure surface, reduces stress concentration within the weak layer, and promotes effective load transfer into stable soil zones, thereby suppressing deep-seated and basal failures. Across both slope types, the observed optimum nail configurations reflect a balance between geometric demand and mobilisation efficiency, confirming the importance of slope-specific reinforcement design and validating the adopted

ISSN: 1311-1728 (printed version); ISSN: 1314-8060 (on-line version)

numerical optimization framework through close agreement with reported literature values.

Table 6: Comparison of unreinforced and reinforced homogeneous soil slopes.

Slope angle (*β*)	**45°**		**60°**	
	Unreinforced	**Reinforced**	Unreinforced	**Reinforced**
Static	1.09	**1.5**	0.8743	**1.509**
Seismic	0.92005	**1.19**	0.76	**1.19**

Table 7: Optimum length and spacing of soil nails.

Slope angle (*β*)	**45°**	**60°**
Length (m)	6.28	6.25
Spacing (m)	1.4	1.2

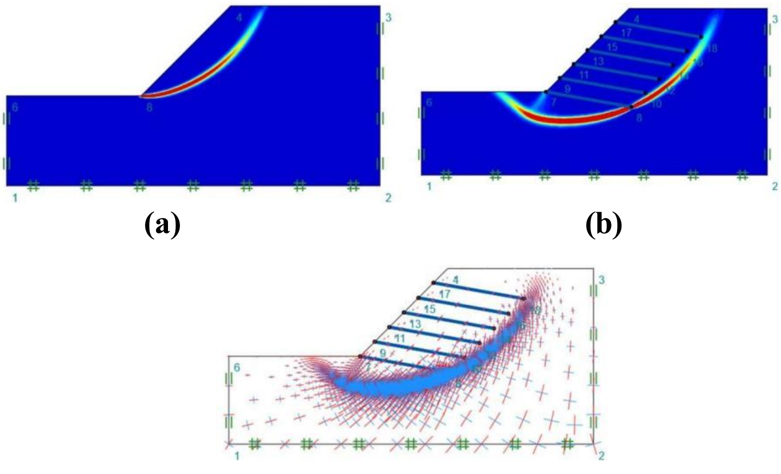

(c)

Figure 14: Failure surface and stress vector diagram of homogeneous static loaded slope (*β*=45°) (a)Unreinforced slope (b)Soil nailed slopes (c) Stress vector diagram

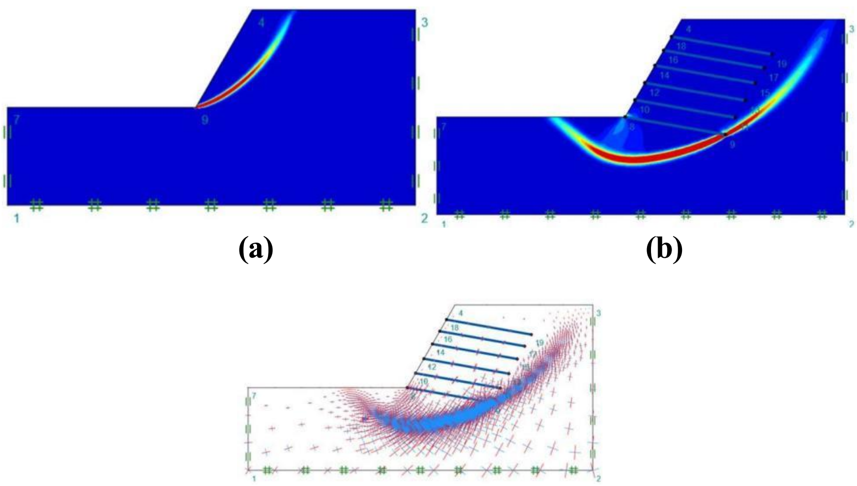

(c)

Figure 15: Failure surface and stress vector diagram of homogeneous static loaded slope (*β*=60°) (a) Unreinforced slope (b) Soil nailed slopes (c) Stress vector diagram

Table 8: Comparison of unreinforced and reinforced layered (*h/t*=0) soil slopes.

ISSN: 1311-1728 (printed version); ISSN: 1314-8060 (on-line version)

Slope angle (*β*)	**45°**		**60°**	
h/t=0	Unreinforced	**Reinforced**	Unreinforced	**Reinforced**
Static	1.0305	**1.504**	0.8162	**1.507**
Seismic	0.9081	**1.1**	0.7430	**1.2**

Table 9: Optimum length and spacing of soil nails.

Slope angle (*β*)	**45°**	**60°**
Length (m)	6.6	6.45
Spacing (m)	1.41	1.1

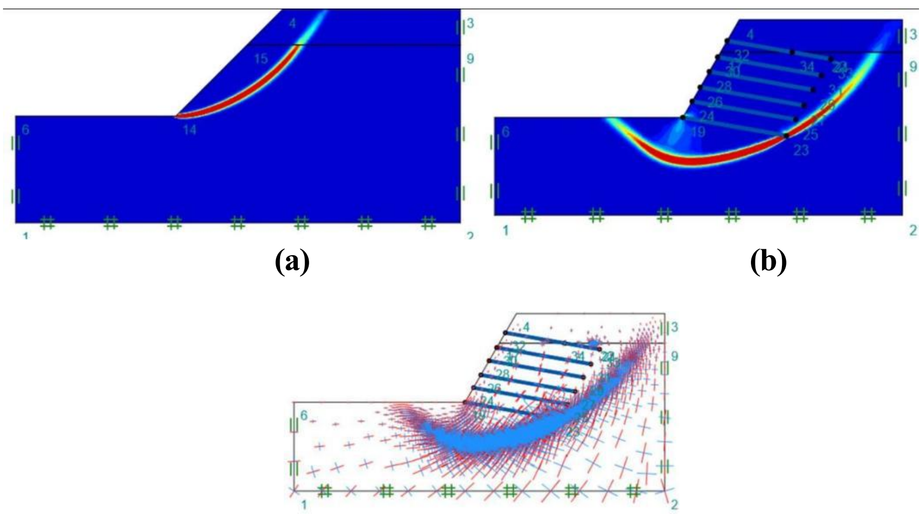

(c)

Figure 16: Failure surface and stress vector diagram of layered static loaded slope (*β*=60° and *h/t*=0) (a) Unreinforced slope (b) Soil nailed slopes (c) Stress vector diagram

5. CONCLUSIONS

This work assessed the stability of homogeneous and layered soil slopes under static and seismic loads using the strength reduction finite element method in OPTUM G2, with emphasis on slope geometry, weak-layer position, constitutive modelling, and soil nailing reinforcement. Results suggest that slope angle is the major geometric factor determining stability, with safety factors dropping consistently as slopes steepen from 30° to 60°, with further decreases happening under seismic loading. For homogeneous slopes, Mohr–Coulomb and Drucker– Prager models offer equivalent findings for moderate slopes but differ for steeper geometries, underscoring the relevance of constitutive model selection approaching failure conditions. In layered slopes, stability is strongly controlled by the position of the thin weak layer, with minimum safety factors observed when the weak layer is located near the lower portion of the slope height, while seismic loading reduces sensitivity to layer position except when the weak layer lies near the slope crest. Soil nailing showed to be a viable stabilization strategy for both slope types, with optimal nail layouts successfully restoring unstable slopes to target safety levels; steeper slopes needed shorter nail lengths and closer spacing due to increasing reliance on reinforcing mobilization. Stress redistribution and shear dissipation patterns verified the function of soil nails in restricting deformation and modifying failure mechanisms. The findings provide practical guidance for the assessment and reinforcement of natural and engineered slopes, support the use of OPTUM G2 as a reliable advanced analysis tool, and highlight the need for future studies incorporating rainfall effects, three-dimensional modelling, and field validation.

The conclusions of this study are directly applicable to the design and assessment of cut slopes, embankments, and hillside infrastructure in layered soils, particularly under seismic circumstances. Identification of crucial weak-layer areas enables more focused site inquiry and efficient reinforcement design, while the proposed soil-nailing configurations offer practical assistance for achieving target safety levels without unnecessary conservatism.

Nomenclature

MC	Mohr-Coulomb
DP	Drucker-Prager
FoS	Factor of safety
FEM	Finite Element Method
SRFEM	Strength Reduction Finite Element Method
β	Soil slope angle

Conflicts of Interest

There is no vested interest for the author.

Acknowledgement

The authors would like to sincerely thanks Department of Civil Engineering, Madan Mohan Malaviya University of Technology, Gorakhpur, Uttar Pradesh, India, for providing access to the use of OPTUM G2 software.

REFERENCES

1. Fawaz, A., Farah, E., & Hagechehade, F. (2014). Slope stability using numerical modelling. *American Journal of Civil Engineering*, **2**(3), 60–67.
2. Abramson, L. W., Lee, T. S., Sharma, S., & Boyce, G. M. (2002). *Slope stability and stabilization* (2nd ed., pp. 329–461). John Wiley & Sons
3. Lin, H., & Cao, P. (2012). Limit equilibrium analysis for the relationships among slope cohesion, friction angle, and slip surface. *Electronic Journal of Geotechnical Engineering*, **17**, 185–195.
4. Namder, A. (2010). *Analysis of slope stability using limit equilibrium methods* (pp. 75– 84). Mysore University, India.
5. Cala, M., & Flisiak, J. (2003). Slope stability analysis with numerical and limit equilibrium methods. In *Proceedings of the 15th International Conference on Computer Methods in Mechanics* (pp. 1–4), Gliwice, Poland.
6. Duncan, J. M. (1996). State of the art: Limit equilibrium and finite element analysis of slopes. *Journal of Geotechnical Engineering*, **122**(7), 577–596.
7. Griffiths, D. V., & Lane, P. A. (1999). Slope stability analysis by finite elements. *Géotechnique*, **49**(3), 387–403.
8. He, B., & Zhang, H. (2012). Stability analysis of slope based on finite element method. *International Journal of Engineering and Manufacturing*, **3**, 70–74
9. Moni, M. M., & Sazzad, M. M. (2015). Stability analysis of slopes with surcharge by limit equilibrium and finite element methods. *International Journal of Advanced Structures and Geotechnical Engineering*, **4**, 216–225.
10. Duncan, J. M., Wright, S. G., & Brandon, T. L. (2014). *Soil strength and slope stability*. John Wiley & Sons
11. Xanthakos, P. P. (1991). *Ground anchors and anchored structures*. John Wiley & Sons.
12. Wu, T. H. (1995). Slope stabilization. In *Slope stabilization and erosion control: A bioengineering approach*. Chapman & Hall

Received: October 25, 2025

13. Lazarte, C. A., et al. (2015). *Geotechnical Engineering Circular No. 7: Soil nail walls—Reference manual*. National Highway Institute, USA.
14. Budania, R., & Arora, R. P. (2016). Soil nailing for slope stabilization: An overview. *International Journal of Engineering Science and Computing*, **6**(12), 3877–3882
15. Federal Highway Administration (FHWA). (1994). *Soil nailing field inspectors manual—Soil nail walls* (Report No. FHWA-SA-93-068). Washington, DC.
16. Taib, S. N. L. (2010). A review of soil nailing design approaches. *Journal of Civil Engineering, Science and Technology*, **1**(2), 1–6.
17. Elias, V., & Juran, I. (1991). *Soil nailing for stabilization of highway slopes and excavations* (FHWA-NHI-00-043). Federal Highway Administration, USA.
18. Babu, G. L. S., & Singh, V. P. (2008). Numerical analysis of performance of soil nail walls under seismic conditions. *ISET Journal of Earthquake Technology*, **45**(1–2), 31– 40.
19. Bathini, D. J., & Krishna, V. R. (2022). Performance of soil nailing for slope stabilization. *IOP Conference Series: Earth and Environmental Science*.
20. Hossain, M. A., & Islam, A. (2016). Numerical analysis of the effects of soil nails on slope stability. *International Journal of Computer Applications*, **141**(8), 12–15.
21. Fan, C. C., & Luo, J. H. (2008). Numerical study on the optimum layout of soil-nailed slopes. *Computers and Geotechnics*, **35**(4), 585–599.
22. Jewell, R. A., & Pedley, M. J. (1992). Analysis for soil reinforcement with bending stiffness. *Journal of Geotechnical Engineering*, **118**(10), 1505–1528.
23. Pham, N. T., Bing, P., & Nguyen, N. V. (2020). Effect of soil nail parameters on the stability of vertical slopes. *Journal of Mining and Earth Sciences*, **61**(6), 30–37
24. Javia, V., et al. (2013). Experimental study on horizontal and inclined soil nails in sand. *Global Research Analysis*, ISSN 2277-8160
25. Villalobos, A. F., Villalobos, A. S., & Orostegui, P. L. (2017). Parametric study of seismic design of soil nailing. *Proceedings of the Institution of Civil Engineers*. https://doi.org/10.1680/jgrim.17.00027
26. Rawat, P., & Chatterjee, K. (2018). Seismic stability analysis of soil slopes using soil nails. *Geotechnical Special Publications*, 79–87
27. Pathak, B. (2023). Analysis of maximum economic length of soil nail for slope stability. *Journal of Earth and Marine Technology*, **4**, 10–17.
28. Wei, W. B., & Cheng, Y. M. (2010). Soil-nailed slopes analyzed by strength reduction and limit equilibrium methods. *Computers and Geotechnics*, **37**, 602–618.
29. Mittal, S., & Biswas, A. K. (2006). River bank erosion control by soil nailing. *Geotechnical and Geological Engineering*, **24**, 1821–1833.
30. Rotte, V., Viswanadham, B., & Chourasia, D. (2011). Influence of slope geometry and nail parameters on soil-nailed slopes. *International Journal of Geotechnical Engineering*, **5**(3), 267–281
31. Gunawan, I., Surjandari, N. S., & Purwana, Y. M. (2017). Study on length-to-diameter ratio of nails for slope stabilization. *IOP Conference Series*, **909**, 012073.
32. Rawat, S., & Gupta, A. K. (2016). Experimental and analytical study of slope stability using soil nailing. *Electronic Journal of Geotechnical Engineering*, **21**(17).
33. Rawat, S., & Gupta, A. K. (2016). Analysis of nailed slopes using limit equilibrium and finite element methods. *International Journal of Geosynthetics and Ground Engineering*, **2**, 34.
34. Sarkar, S., & Chakraborty, M. (2021). Stability analysis of two-layered slopes using strength reduction method. *International Journal of Geo-Engineering*, **12**, 24.
35. Chatterjee, D., & Murali Krishna, A. (2018). Stability analysis of two-layered non- homogeneous slopes. *International Journal of Geotechnical Engineering*, 1–7
36. Sazzad, M. M., & Mazumder, S. (2015). Seismic stability analysis of homogeneous and layered soil slopes using LEM. *International Journal of Computer Applications*, **117**, 12–17.

Volume 38 No. 10s, 2025
ISSN: 1311-1728 (printed version); ISSN: 1314-8060 (on-line version)

37. Sazzad, M. M., & Moni, M. M. (2017). Stability analysis of homogeneous and layered soil slopes using FEM. *Journal of Engineering Science*, **8**, 51–62
38. Optum G2. (2017). *Optum computational engineering software*. Copenhagen, Denmark.
39. Altalhe, E. B., & Abdalftah, H. (2019). Stability of nailed sand slopes and anchored length effects. *International Conference on Technical Sciences (ICST 2019)*, p. 40.

Received: October 25, 2025